

Endocrine disrupter compounds removal in wastewater using

microalgae: Degradation kinetics assessment

M.R. Abargues^a, J. B. Giménez^a, J. Ferrer^b, A. Bouzas^{a,*}, A. Seco^a.

^aCALAGUA – Unidad Mixta UV-UPV, Departament d'Enginyeria Química, Universitat de València, Avinguda de la Universitat s/n, 46100 Burjassot, Valencia, Spain.

^bCALAGUA – Unidad Mixta UV-UPV, Institut Universitari d'Investigació d'Enginyeria de l'Aigua i Medi Ambient – IIAMA, Universitat Politècnica de València, Camí de Vera s/n, 46022 Valencia, Spain.

E-mail addresses: miguel.abargues@uv.es (M.R. Abargues), Juan.B.Gimenez@uv.es (J.B. Giménez), jferrer@hma.upv.es (J. Ferrer), alberto.bouzas@uv.es (A. Bouzas), aurora.seco@uv.es (A. Seco).

Abstract

This paper describes a study carried out to determine the removal kinetics of four micropollutants (4-tert-octylphenol (OP), technical-nonylphenol (t-NP), 4-nonylphenol (4-NP) and bisphenol-A (BPA)) usually found in wastewater streams. The kinetic experiments were carried out in batch reactors containing the effluent of an Anaerobic Membrane BioReactor (AnMBR) in the presence of light, oxygen and microalgae. As the degradation process of the studied micropollutants obeyed a pseudo-first-order kinetics, the second-order kinetics for each micropollutant was then calculated. The second order rate constants for the hydroxyl radical (k_{OH}) ranged from $7.0 \cdot 10^{+10}$ to $6.6 \cdot 10^{+12}$ L·mol⁻¹·min⁻¹ and for the oxygen (k_{O_2}) from 77 to 125 L·mol⁻¹·min⁻¹. The k_{O_2} values were significantly lower than the k_{OH} values, indicating that the hydroxyl radical is a better oxidising agent than oxygen. However, as the concentration of

* Corresponding author. Tel.: +34 96 354 45 41.

dissolved oxygen was higher than that of the hydroxyl radical, higher oxygen pseudo-first order rate constants were produced (k'_{O_2} , ranging from 0.016 to 0.026 min^{-1}) than hydroxyl radical pseudo-first order rate constants ($k'_{\cdot OH}$, ranging from $7.0 \cdot 10^{-05}$ to $6.6 \cdot 10^{-03}$ min^{-1}), bringing the degradation process under the control of the oxygen mechanism. The proposed kinetic model was validated by fitting experimental data from a study of supersaturated oxygen concentration and showed good correlation for all the studied micropollutants.

Keywords

Degradation kinetics; endocrine disruptor; hydroxyl radical, microalgae; oxygen; wastewater.

1. Introduction

A number of common micropollutants have been detected in natural environments, mainly from manufactured products, such as surfactants and pesticides or plastic reinforcements [1]. As some of these chemicals are able to disrupt the endocrine system they are known as *endocrine disruptor compounds* (EDCs) [2]. EDCs are now a global concern due to their widespread occurrence, persistence, and bioaccumulation, although they can be removed in wastewater treatment plants (WWTPs) [3, 4]. 4-tert-octylphenol (OP) and technical-nonylphenol (t-NP) are known as alkylphenol (APs) and both are degradation metabolites of alkylphenol polyethoxylates (APEOs), used in detergents, paints, and resins, among other commercial products [5]. APs are more toxic than APEOs because they are more lipophilic and can spread to humans via the food chain as they accumulate in fish and birds [6]. Although 4-nonylphenol (4-NP) is an alkylphenol, it is not an APEO metabolite, seldom occurs in the environment [7, 8] and biodegrades faster than OP and t-NP [9, 10]. Bisphenol-A (BPA) is used to produce epoxy resins and polycarbonate plastics and can interfere in cell division mechanisms and mimic female oestrogen 17 β -Estradiol [5, 11].

European Directive 2000/60/EC [12], also known as the Water Framework Directive (WFD) was designed to protect surface, subterranean, transitional and coastal waters.

Directives 2008/105/EC [13] and 2013/39/EU [14], amending the WFD, laid down environmental quality standards (EQS) for priority substances and certain other pollutants, such as OP, 4-NP and t-NP, and included BPA as a substance subject to be reviewed for possible identification as a priority substance. The removal of these substances in WWTPs would therefore ensure the protection of bodies of water that receive wastewater discharges.

Anaerobic Membrane Bioreactors (AnMBR) are considered as a sustainable approach for organic matter removal in low-strength wastewaters [15]. However, the high nitrogen and phosphorus concentrations in AnMBR effluents often prevent their being discharged into aquatic environments without further nitrogen and phosphorus removal. Mixed microalgal culture systems have been shown to be feasible treatments for nutrient removal from AnMBR effluents [16]. Besides the aforementioned classical pollutants, priority substances and their metabolites must now be taken into account when assessing wastewater treatment efficiency [4, 17]. A previous work [18] assessed OP, t-NP, 4-NP and BPA removal efficiency by means of microalgae in AnMBR effluent, but provided no information on the removal kinetics. Many studies on degradation process kinetics assumed simple first-order for OP, nonylphenols and BPA [19, 20]. However, other authors have created a pseudo-first order kinetics model for these micropollutants [21] or even a zero-order kinetics in a catalysed reaction [22].

The aim of this research project was thus to determine the removal kinetics of four micropollutants (OP, t-NP 4-NP and BPA), classified as EDCs, evaluating different parameters involved in a microalgae wastewater treatment such as light, oxygen and microalgae. The degradation experiments combining the studied variables were carried out in batch reactors fed with AnMBR effluent.

2. Materials and methods

2.1. Reagents, solutions and microalgae culture

4-nonylphenol (4-NP) (CAS Number 104-40-5) and technical-nonylphenol (t-NP) (CAS Number 84852-15-3) were obtained from Riedel-de Haën (Seelze, Germany). 4-tert-octylphenol (OP) (CAS Number 140-66-9) and Bisphenol-A (BPA) (CAS Number 80-05-7) were purchased from Sigma-Aldrich (Steinheim, Germany). All the reagents were of analytical grade.

Acetonitrile was purchased from Sigma-Aldrich (Steinheim, Germany). Pure water was obtained by means of a Synergy UV purification system purchased from Milli-Q (Millipore, Billerica, MA, USA). Helium and carbon dioxide were purchased from Carbueros Metálicos (Barcelona, Spain).

The stock solutions of standards were prepared in acetonitrile up to a maximum concentration of 1000 mg/L. The more dilute solutions were prepared from stock solutions directly in pure water up to a maximum concentration of 1 mg/L. All the solutions were kept at 4 °C until use.

The microalgae used as inoculum were obtained from the walls of the secondary clarifier of the Carraixet WWTP (Valencia, Spain) and kept in the laboratory in a semi-continuous reactor operated at a low retention time (<2d), fed with the AnMBR effluent and under continuous illumination. PAR was measured in this reactor and gave values between 114 and 198 $\mu\text{E}\cdot\text{m}^{-2}\cdot\text{s}^{-1}$. Microalgae from the *Chlorococcales* order of the *Chlorophyceae* class were identified as the main group present, together with *cyanobacteria*. The medium was adjusted to pH 7.2-7.5 by CO_2 .

2.2. Fractional factorial design

The oxygen, light and microalgae parameters (three variables taking part in microalgae wastewater treatments) were evaluated to obtain the rate law, rate constant and half-life of

the degradation reaction of each micropollutant studied. The effect of oxygen, light and microalgae on their degradation rate was tested by a factorial experimental design. The full factorial design [23] requires all combinations of the studied levels (n) of each of variable (f) (i.e., $n=2$; presence (+) or absence (-) of the three studied variables, $f=3$; oxygen, light and microalgae). The total number of experiments for the design would be $8 (n^f)$, which corresponds to three variables (oxygen, light and microalgae) and two levels per variable, however the eight experiments were reduced to the five shown in Table 1. The experiments with the microalgae variable and without the light variable were discarded, since microalgae growth is inhibited under these conditions. Moreover, the experiment without the presence of any of the three studied variables was considered as a control experiment. No degradation was observed in this control experiment and therefore it was also excluded from the study.

2.3. Experimental set-up

The kinetic degradation study was carried out in the reaction system shown in Figure 1, which consisted of five Pyrex® batch reactors of 2.0 L of total volume, with the work volume set at 1.6 L. The reactors were fed with 800 mL of aerated AnMBR effluent (see [15] for a detailed AnMBR pilot plant description). The remaining 800 mL were filled with raw microalgae culture for the POM and PM experiments, or 800 mL of pure water for the PO, P and O experiments. All the experiments were carried out inside a walk-in climatic chamber (Ineltec, Barcelona, Spain), at 23.5 ± 0.5 °C. The experiments under forced aeration (POM, PO and O) were aerated and agitated by means of a compressor connected to a diffuser at the bottom of the reactor. The experiments under non-aerated conditions (PM and P) were agitated at 100 rpm for homogenisation. In the experiment with microalgae culture (POM), a carbon dioxide stream was used to keep pH between 7.2 and 7.5. The illuminated experiments were irradiated by four fluorescent 18 W lamps obtaining a photosynthetically active radiation (PAR) of $135 \mu\text{E}/\text{m}^2 \cdot \text{s}$. A detailed description of the set-up can be found in [18].

Each reactor was spiked with 5.6, 24.0, 16.0 and 16.0 μg of OP, t NP, 4-NP and BPA, respectively. The fortification chosen was 5 times the average concentration of the pilot plant AnMBR effluent for each micropollutant [9].

The average wastewater characteristics of the AnMBR effluent during the studied period were: $63.6 \pm 0.2 \text{ mg COD/L}$, $39 \pm 4 \text{ mg BOD/L}$, $46.3 \pm 0.6 \text{ mg NH}_4^+\text{-N/L}$, $6.2 \pm 0.2 \text{ mg PO}_4^{3-}\text{-P/L}$, $14.3 \pm 0.3 \text{ mg SO}_4^{2-}\text{-S/L}$, $109 \pm 8 \text{ mg S}^{2-}\text{/L}$, $665 \pm 10 \text{ mg CaCO}_3\text{/L}$ of Alkalinity, and the Volatile Fatty Acids remained close to zero. The chemical and microbiological characteristics of the POM reactor are shown in SM1 and SM2, respectively.

2.4. Analytical Methods

The solid-phase microextraction (SPME) coupled with gas chromatography/mass spectrometry (GC/MS) method was adapted from [24]. Briefly, the SPME procedure was carried out with 20 mL samples placed in a 20 mL clear vial screw top (Supelco, Bellefonte, PA, USA) with a magnetic stir bar (VWR International Eurolab, Barcelona, Spain). A polyacrylate (PA) fibre (Supelco, Bellefonte, PA, USA) was mixed into the sample by constant stirring (1500 rpm) for 60 min. The fibre was immediately removed and placed in the injection port of the GC/MS for 15 s for micropollutant desorption.

In order to analyse the POM and PM experiments, 40 mL of the batch reactor mixed liquor were centrifuged at 5000 rcf for 5 min. 20 mL of supernatant were placed in a 20 mL vial and analysed by the SPME/GC/MS technique.

All the analyses were performed on a gas chromatography-mass spectrometry system (GC/MS) using 6890N GC with 5973 inert MS Detector (Agilent, Palo Alto, CA, USA) equipped with a split/splitless injection port and operated by MSD Productivity Chemstation SW D.01.02 Software (Agilent, Palo Alto, CA, USA). The capillary column was a fused-silica HP-5ms Ultra Inert (30.0 m, 250 μm I.D., 0.25 μm film thickness) (Agilent, Palo Alto, CA, USA).

The MS worked in the selected-ion-monitoring mode (SIM) and the electron impact energy was set to 69.9 eV. The GC/MS was operated in splitless mode and the injection port and the ion source temperature were held isothermally at 280 and 250 °C, respectively. The temperature program used was as follows: initial temperature of 50 °C, 30 °C/min to 140 °C, held for 1 min, 20 °C/min to 280 °C, held for 4 min, 30 °C/min to 310 °C, held for 2 min, for a total run time of 19 min. Helium was used as carrier gas with a constant flow of 1.0 mL/min.

A Mettler-Toledo microbalance XP105 Delta Range (Greifensee, Switzerland) with a resolution of 0.01 mg was used for weighing standards. An Eppendorf centrifuge 5804R (Brinkmann Instruments, Westbury, NY, USA) was used to separate the suspended and soluble fractions. The PAR was determined using a HOBO Photosynthetic Light Smart Sensor and HOBO Micro Station Data Logger (MicroDAQ.com Ltd, Contoocook, NH, USA). The dissolved oxygen concentration was measured by an OxiCal-SL CelIOx 325 probe (WTW, Weilheim, Germany), connected to a Multi 340i meter (WTW, Weilheim, Germany). The pH was measured by WTW SenTix 41 probe (WTW, Weilheim, Germany), connected to a Consort pH Meter model C861 (Turnhout, Belgium).

The GC/MS system was operated in full scan mode (scan range from 100 to 300 m/z) to find the characteristic ions and the relative abundance of each compound studied. Chemical structure, octanol-water partition coefficient (K_{ow}), Retention time, Quantification and Characteristic Ions of the analysed compounds are shown in Supplementary Material SM3. Some of the characteristic ions were confirmed by the NIST library (Gaithersburg, Maryland, USA).

The quality assurance parameters such as detection and quantification limits, precision and linearity were evaluated in the selected ion monitoring (SIM) mode. The values of these parameters are described in [18].

2.5. Kinetics analysis

The overall micropollutant degradation rate is due to three processes: chemical oxidation, biodegradation and sorption [25]. A previous study has pointed out that chemical oxidation seems to be the most effective mechanism in micropollutant degradation [18], since oxygen is necessary for attacking the aromatic rings. Under the experimental conditions detailed in Table 1 (illuminated and aerated reactors with a microalgae culture), chemical oxidation could be considered as the main process, due to the high level of dissolved oxygen (higher than 8 mg O₂/L for POM, PO, O and PM experiments and 1.7 mg O₂/L for P experiment). As chemical oxidation consists of oxygen or radical oxidation [26, 27] both oxidation mechanisms were studied in this work. Oxygen is added to the system or generated inside the system, whereas radicals are generated in situ by the action of light on the chemical species contained in the matrix. Free radicals are most often formed by photochemical reactions in which the light energy is capable of exciting chemical species, such as nitrate ion, hydrogen peroxide or dissolved organic matter, generating free radicals as reaction products. Hydroxyl ($\cdot\text{OH}$), carbonate ($\cdot\text{CO}_3^-$), and peroxide ($\cdot\text{OOH}$) radicals are the most common free radicals. Figure 2 shows schematically the formation reactions of the aforementioned radicals.

The hydroxyl radical is generated in three ways: irradiation of nitrate ion, hydrogen peroxide and organic matter. The irradiation of nitrate in its long-wavelength absorption band (wavelength below 302 nm) results in two primary photochemical processes [26, 27, 28]. Reaction 1 appears as the nitrate ion is excited by light and is transformed into radical $\cdot\text{O}^-$, the precursor of the hydroxyl radical [19, 28]. As Reaction 2 shows, radical $\cdot\text{O}^-$ is rapidly protonated to its conjugated acid, the hydroxyl radical. Even so, the fate of the atomic oxygen produced in Reaction 1 is likely to react with molecular oxygen to form ozone [28]. As Reaction 3 shows, the cleavage of one hydrogen peroxide molecule produces two molecules of hydroxyl radical [29]. The third way for hydroxyl radical formation is through irradiation of dissolved organic matter (DOM) in the presence of oxygen. The overall chemical mechanism is shown in

Reaction 4. As can be observed, hydrogen peroxide is produced after irradiation of dissolved organic matter, which, as mentioned above, produces a hydroxyl radical in the presence of light.

The carbonate radical (CO_3^-) is a product of the reaction between carbonate or bicarbonate and a hydroxyl radical that takes place without light. The overall chemical mechanism is shown in Reaction 5.

Finally, peroxide radicals ($\cdot\text{OOH}$) are formed in three stages: reaction between the hydroxyl radical and dissolved organic matter with unsaturated carbon-carbon bonds; reaction with molecular oxygen; and finally cleavage of the peroxide radical group ($\cdot\text{OOH}$). Reaction 6 shows an example of this mechanism [30].

Both peroxide and carbonate radicals are known to react selectively with sulphur-containing compounds, whereas the hydroxyl radical is a strong and non-selective oxidant that rapidly reacts with organic chemicals [31]. The oxidation potential of the hydroxyl radical is thus higher than the carbonate and hydrogen peroxide radicals [26].

Although many published degradation studies assume simple first-order degradation kinetics in oxidation processes [19, 20, 25], second order kinetics was considered for all the degradation processes in this work. In the presence of oxidants, the degradation mechanism of the studied micropollutants can be described by the sum of the second order kinetics of each oxidation process, each of them having its own reaction rate. The global degradation process can be expressed as in Eq. (1).

$$-d[A]/dt = k_{\text{O}_2} \cdot [\text{O}_2] \cdot [A] + k_{\cdot\text{OH}} \cdot [\cdot\text{OH}] \cdot [A] \quad (1)$$

where, $[A]$, $[\cdot\text{OH}]$ and $[\text{O}_2]$ are the micropollutant, hydroxyl radical and dissolved oxygen concentrations (mol/L), k_{O_2} is the oxygen second order degradation rate constant ($\text{L}\cdot\text{mol}^{-1}\cdot\text{min}^{-1}$) and $k_{\cdot\text{OH}}$ is the hydroxyl radical second order degradation rate constant ($\text{L}\cdot\text{mol}^{-1}$

$^1 \cdot \text{min}^{-1}$). In order to simplify the experiments and the mathematical calculation, Eq. (1) can be transformed from second-order kinetics to pseudo-first-order kinetics, using a constant concentration of oxidant agent ($[\cdot\text{OH}]$ and $[\text{O}_2]$). Thus, each degradation rate constant from Eq. (1) can be expressed as in Eq. (2).

$$k'_i = k_i \cdot [\text{Ox}]_e \quad (2)$$

where $[\text{Ox}]_e$ is the steady state oxidant concentration (mol/L), k_i is the second order degradation rate constant ($\text{L} \cdot \text{mol}^{-1} \cdot \text{min}^{-1}$) and k'_i the pseudo-first order rate constant for each degradation mechanism (min^{-1}).

The observed rate constant (k_{obs}) can be expressed as the sum of each degradation rate constant Eq. (3).

$$k_{\text{obs}} = k'_{\text{O}_2} + k'_{\text{OH}} = k_{\text{O}_2} \cdot [\text{O}_2] + k_{\text{OH}} \cdot [\cdot\text{OH}] \quad (3)$$

where k_{obs} is the sum of both pseudo-first-order rate constants (k'_{O_2} and k'_{OH}) (min^{-1}).

Hence, using Eq. (2) and (3), Eq.(1) can be simplified to Eq. (4) and (5).

$$-d[A]/dt = (k'_{\text{O}_2} + k'_{\text{OH}}) \cdot [A] \quad (4)$$

$$\text{Ln}([A]_t/[A]_0) = k_{\text{obs}} \cdot t \quad (5)$$

where, $[A]_t$ is the micropollutant concentration existing at time t (mol/L) and $[A]_0$ is the initial micropollutant concentration (mol/L). The pseudo-first-order rate constant was evaluated by plotting $\text{Ln}([A]_t/[A]_0)$ vs time. The half-life ($t_{1/2}$, min) of each micropollutant can thus be expressed as in Eq. (6).

$$t_{(1/2)} = \text{Ln}2/(k_{\text{obs}}) \quad (6)$$

3. Results and discussion

The above-mentioned second-order kinetics can be simplified to pseudo-first-order kinetics if the dissolved oxygen and hydroxyl radical concentrations remain constant during the kinetic experiment. The AnMBR effluent fed to the reactors had a high ammonium concentration (46.3 ± 0.6 mg NH_4^+ -N/L), which under the trial's aerobic conditions was partially oxidized to nitrate. As can be observed in Table 1, the nitrate concentration was nearly constant throughout the experiment. The organic matter concentration (COD) in the AnMBR effluent was not metabolised by the microalgae culture used in the study, keeping practically constant during the experiment as shown in Table 1. Previous experiments [16] showed that this COD corresponds mainly to non-biodegradable soluble organic matter for algae. The hydroxyl radical therefore can be considered constant in the reaction medium, since its precursors (nitrate and dissolved organic matter) were constant. The dissolved oxygen concentration (Table 1) could also be considered stable during the experiment, so that the kinetics can be simplified to a pseudo-first order.

In all the experiments, samples were taken on the following basis: every 20 min between 0 and 100 min, every 30 min between 100 and 220 min and every 1440 min from 220 min until the end of the experiment. Although the experiments lasted 72 hours, data exceeding 165 min were not necessary to adequately fit the kinetics mechanisms. The micropollutant concentrations in the reactors were monitored in order to compare the different system dynamics. The normalized concentrations of the micropollutants (C/C_0) were plotted against time.

3.1. Degradation kinetics in O, P, PO and POM experiments

The experimental conditions in the O, P, PO and POM experiments are given in Table 1. The P experiment was carried out in a reactor previously bubbled with nitrogen for 30 min to reduce the dissolved oxygen concentration to 1.7 ± 0.2 mg O_2 /L.

As shown in Figure 3, two stages can be observed in micropollutant degradation in aerated conditions. After an initial stage characterised by a faster degradation rate (approximately 60 min reaction time), the process degradation rate dropped rapidly, which can be attributed to the drastic reduction of the micropollutant concentration. The micropollutant degradation profile in the non-aerated experiment (P) is shown in Figure 4, where it can be seen that experiment P lacks the two stages observed in the aerated experiments and has an almost constant degradation trend.

In order to obtain the degradation kinetics and the rate constants of the micropollutants, the data were fitted into a pseudo-first-order kinetics model according to Eq. (5). This model seems to accurately describe the kinetic process, since the correlation coefficients (r^2) are higher than 0.98 and the calculated half-lives ($t_{1/2}$) match the experimental data (see Table 2 and Figure 3).

As seen in Table 2, the micropollutant degradation kinetics is similar in the three aerated experiments (O, PO, and POM). Although some authors have reported that the humic and fulvic acids produced during algae decomposition can accelerate photodegradation since they act as photosensitizers [32, 33, 34], this was not detected in the POM results. The k_{obs} values in the POM and PO experiments were similar, except for BPA, which showed a lower k_{obs} value in the POM experiment. The k_{obs} values in experiment O were lower than the k_{obs} in POM and PO for OP and t-NP, showing that light is an important parameter in OP and t-NP degradation.

The rate constants in experiment P (Table 2) are considerably lower than those obtained for POM, PO and O, which points to a lower degradation efficiency under non-aerated conditions. 4-NP also showed the lowest half-life in the P experiment, indicating that this is the most degradable compound in non-aerated processes.

Once the k_{obs} values were determined, the pseudo-first order kinetics (k'_{O_2} , see Table 3) and the second order degradation rate constants (k_{O_2} , see Table 3), for the oxygen mechanism were calculated by Eqs. (2) and (3). As the O experiment was carried out without light, Eq. (3) can be simplified to Eq. (7), thus both k_{obs} and k'_{O_2} have the same value in experiment O, so that the k_{O_2} value in this experiment can be calculated for each micropollutant with dissolved oxygen and consequently the k_{obs} (Table 2) values. As described below, the k'_{O_2} and k_{O_2} for POM and PO experiments were determined by Eq. (3), so that k'_{OH} and k_{OH} rate constant values were necessary.

$$k_{obs} = k'_{O_2} = k_{O_2} \cdot [O_2] \quad (7)$$

Once the k_{O_2} values for O experiment are determined, k'_{OH} and k_{OH} can be calculated by means of Eq. (3) for the P experiment. The hydroxyl radical concentration required in Eq. (3) could not be measured and so a value was selected from the literature. Ryan et al. [35] determined that the hydroxyl radical concentration in an aerobic process effluent, with a nitrate concentration (hydroxyl radical precursor) between 0.1 and 4.2 mg NO_3^- -N/L, ranged from 10^{-15} to 10^{-14} mol/L. Similar values have been found in surface waters by others authors [25, 26]. The average nitrate concentration in the POM, PO, P and O experiments ranged from 2.9 to 3.5 mg NO_3^- -N/L, hence a 10^{-15} mol/L hydroxyl radical concentration was used. The pseudo-first-order rate constant for the hydroxyl radical degradation (k'_{OH}) ranged from 0.00007 to 0.0066 min^{-1} (Table 3), and the second order rate constant for the hydroxyl radical degradation (k_{OH}) ranged from $7.0 \cdot 10^{+10}$ to $6.6 \cdot 10^{+12}$ $L \cdot mol^{-1} \cdot min^{-1}$ (Table 3). The k'_{OH} and k_{OH} constants were only calculated in the P experiment, because it had the lowest dissolved oxygen concentration and therefore the lowest k_{OH} error.

The k'_{O_2} and k_{O_2} values for the POM and PO experiments were obtained by Eq. (3), the k'_{OH} and k_{OH} values calculated for the P experiment and the hydroxyl radical and dissolved oxygen concentrations. The average k_{O_2} value for each micropollutant obtained from the

aerated experiments (POM, PO and O) is shown in Table 3, in which the second order rate constant (k_{O_2}) ranges from 87 to 125 L·mol⁻¹·min⁻¹.

The k_{O_2} values are significantly lower than the k_{OH} values, indicating that the hydroxyl radical is a better oxidising agent than oxygen. However, as the dissolved oxygen concentration (ca. 10⁻⁰⁴ mol/L) is higher than the hydroxyl concentration (ca. 10⁻¹⁵ mol/L), this leads to higher oxygen pseudo-first-order rate constants (k'_{O_2}) than hydroxyl radical pseudo-first-order rate constants (k'_{OH}), and the degradation process is therefore controlled by the oxygen mechanism.

3.2. Degradation by natural oxygenation of algae

An illuminated microalgae culture experiment (PM) without forced aeration was designed to determine the natural production of dissolved oxygen by microalgae activity and its influence on micropollutant degradation, with a poorly agitated reactor to avoid oxygen stripping. As in the previous experiments, the reactor was maintained at 23.5±0.5°C. The chemical and microbiological characteristics of the PM reactor are shown in SM4 and SM5, respectively.

Figure 5 shows the dissolved oxygen concentration profile in the PM experiment. The initial dissolved oxygen concentration (8.2 mg O₂/L) dropped rapidly due to the sulphide reacting with oxygen to produce sulphate. Once the sulphide was consumed, the dissolved oxygen concentration gradually rose again from the effect of microalgae metabolism and surface reaeration exceeding the oxygen saturation value (7.52 mg O₂/L at 23.5±0.5 °C and 101.325 kPa). The supersaturated conditions were due to the fact that the reaction medium was poorly agitated (100 rpm). Between 141 and 146 h, the dissolved oxygen concentration remained constant (14.7±0.3 mg O₂/L). After 0.5 h (at 141.5 h), the reactor (1.6 L) was spiked with 5.6, 24.0, 16.0 and 16.0 µg of OP, t-NP, 4-NP and BPA respectively. The first sample was collected at 141.5 h, and the rest every 10 minutes. Figure 6 shows the degradation efficiency

of the micropollutants during the sampling period, with faster degradation than in the POM, PO, O and P experiments (Figure 3). This can also be observed in Table 4, which shows the k_{obs} for the PM experiment. These values were higher than the k_{obs} for POM, PO, O and P experiments. The degradation rate of a system with a dissolved oxygen concentration above the saturation value was thus higher than the degradation rate observed under non-supersaturated conditions.

In the PM experiment, the k_{O_2} values were obtained from the k_{obs} value using Eq. (3) and the k'_{OH} value obtained in the previous section. The values obtained were 110.8, 109.7, 82.8 and 93.4 L·mol⁻¹·min⁻¹ for OP, t-NP, 4-NP and BPA, respectively. These values are in line with those obtained in the previous experiments (Table 3).

3.3. Kinetic constants validation

The proposed kinetic model was validated by means of the second order kinetics constants (k_{O_2} and k_{OH} , Table 3) obtained in the calibration step, under the experimental conditions of the PM experiment. Eq. (8) was used to study the kinetic model.

$$[A]_t/[A]_0 = e^{-k_{obs} \cdot t} \quad (8)$$

where $[A]_t$ is the micropollutant concentration at a specific time (mol/L), $[A]_0$ is the micropollutant concentration at initial time (mol/L) and k_{obs} is the observed rate constant under validation conditions (min⁻¹).

The k_{obs} value for the PM experiment was calculated using the k_{O_2} and k_{OH} values and standard deviations shown in Table 3

and the experimental dissolved oxygen and hydroxyl radical concentrations (i.e., 14.7 mg O₂/L and a of 10⁻¹⁵ mol/L, respectively). The validation graphs were developed using the following k_{obs} values:

$$k_{obs,1} = (k_{O_2} + s.d.) \cdot [O_2] + k_{OH} \cdot [\cdot OH]$$

$$k_{obs,2} = k_{O_2} \cdot [O_2] + k_{OH} \cdot [\cdot OH]$$

$$k_{obs,3} = (k_{O_2} - s.d.) \cdot [O_2] + k_{OH} \cdot [\cdot OH]$$

Figure 7 show the experimental data obtained in the PM experiment and the predictions of the fitted model for OP, t-NP, 4-NP and BPA, respectively.

The experimental OP and t-NP data show the good correlation between all the predicted and experimental values (from 0 to 80 min). It can be observed that at low reaction times (between 20 and 30 min) the predicted values of 4-NP and BPA are above the experimental ones, although in general the kinetic model is able to reproduce the micropollutant degradation.

4. Conclusions

The degradation kinetics of OP, t-NP, 4-NP and BPA, commonly detected in AnMBR effluents, was studied using a combination of light, oxygen and microalgae. Two parallel degradation kinetics mechanisms were observed: degradation under dissolved oxygen mechanism and under the hydroxyl radical mechanism. Although the results indicated that the hydroxyl radical was a better oxidant than dissolved oxygen, the low hydroxyl radical concentration in the wastewater meant that the degradation kinetics was controlled by the oxygen mechanism. In the aerated experiments the micropollutant degradation kinetics was similar, observing that light is an important parameter in OP and t-NP degradation. The rate constants under non-aerated conditions were lower than those obtained for aerated conditions. High dissolved oxygen concentrations produced by algae enhanced the degradation rates. The experimental data and the proposed kinetic model gave high correlations of the studied micropollutants, showing that this kinetic model is suitable for predicting OP, 4-NP, t-NP and BPA degradation.

Acknowledgements

This research work was supported by the Spanish Ministry of Economy and Competitiveness (MINECO, CTM2011-28595-C02-01 and CTM2011-28595-C02-02) jointly with the European Regional Development Fund (ERDF), which are gratefully acknowledged.

References

- [1] Birkett J.W., Lester J.N., (2003). Endocrine Disrupters in Wastewater and Sludge Treatment Processes. CRC Press LLC, Florida.
- [2] Lintelmann J., Katayama A., Kurihara N., Shore L., Wenzel A. (2003). Endocrine Disruptors in the Environment (IUPAC Technical Report). Pure Appl. Chem., 75, 631–681
- [3] Liu J., Lu G., Xie Z., Zhang Z., Li S., Yan Z. (2015). Occurrence, bioaccumulation and risk assessment of lipophilic pharmaceutically active compounds in the downstream rivers of sewage treatment plants. Sci. Total Environ. 511, 54–62
- [4] Mamo J., García-Galán M.J., Stefani M., Rodríguez-Mozaz S., Barceló D., Monclús H., Rodríguez-Roda I., Comas J. (2017) Fate of pharmaceuticals and their transformation products in integrated membrane systems for wastewater reclamation. Chem. Eng. J. <http://dx.doi.org/10.1016/j.cej.2017.08.050>
- [5] Sharma V. K., Anquandah G. A. K., Yngard R. A., Kim H., Fekete J., Bouzek K., Ray A. K., Golovko D. (2009). Nonylphenol, octylphenol, and bisphenol-A in the aquatic environment: A review on occurrence, fate, and treatment. J. Environ. Sci. and Health Part A 44, 423-442
- [6] Manente L., Sellitti A., Lucariello A., Laforgia V., De Falco M., De Luca A. (2011). Effects of 4-nonylphenol on proliferation of AGS gastric cells. Cell Prolif. 44, 477–485
- [7] Tanghe T., Dhooge W., Verstraete W. (1999). Isolation of a Bacterial Strain Able To Degrade Branched Nonylphenol. Appl. Environ. Microbiol. 65, 746–751
- [8] De Weert J., Viñas M., Grotenhuis T., Rijnaarts H., Langenhoff A. (2010). Aerobic nonylphenol degradation and nitro-nonylphenol formation by microbial cultures from sediments. Appl. Microbiol. Biotechnol. 86, 761–771

[9] Abargues M. R., Robles A., Bouzas A., Seco A. (2012). Micropollutants removal in an anaerobic membrane bioreactor and in an aerobic conventional treatment plant. *Water Sci. Technol.* 65, 2242-2250

[10] Porter A.W., Campbell B.R, Kolvenbach B.A., Corvini P.F.X., Benndorf D., Rivera Cancel G., Hay A.G. (2012). Identification of the flavin monooxygenase responsible for ipso substitution of alkyl and alkoxyphenols in *Sphingomonas* sp. TTNP 3 and *Sphingobium xenophagum* Bayram. *Appl. Microbiol. Biotechnol.* 94, 261–272

[11] Gattullo C.E., Bährs H., Steinberg C.E.W., Loffredo E. (2012). Removal of bisphenol A by the freshwater green alga *Monoraphidium braunii* and the role of natural organic matter. *Sci. Total Environ.* 416, 501–506

[12] European Commission, 2000. Directive 2000/60/EC of the European Parliament and of the Council of 23 October 2000 establishing a framework for Community action in the field of water policy. *Official Journal of the European Union* L327, 1-77

[13] European Commission, 2008. European Parliament and Council, Directive 2008/105/EC of the European Parliament and of the Council of 16 December 2008 on environmental quality standards in the field of water policy, amending and subsequently repealing Council Directives 82/176/EEC, 83/513/EC, 84/156/EEC, 84/491/EEC, 86/280/EEC and amending Directive 2000/60/EC of the European Parliament and of the Council. *Official Journal of the European Union* L348, 84-97

[14] European Commission, 2013. The Directive 2013/39/EU of The European Parliament and of the Council of 12 August 2013 amending Directives 2000/60/EC and 2008/105/EC as regards priority substances in the field of water policy. *Official Journal of the European Union* L226, 1-17

[15] Giménez J.B., Robles A., Carretero L., Durán F., Ruano M.V., Gatti M.N., Ribes J., Ferrer J., Seco. A. (2011). Experimental study of the anaerobic urban wastewater treatment in a submerged hollow-fibre membrane bioreactor at pilot scale. *Bioresour. Technol.* 102, 8799–8806

[16] Ruiz-Martinez, A., Martin Garcia, M., Romero, I., Seco, A., Ferrer, J. (2012). Microalgae cultivation in wastewater: Nutrient removal from anaerobic membrane bioreactor effluent. *Bioresour. Technol.* 126, 247-253

[17] Xiao Y., Yaohari H., De Araujo C., Sze C.C., Stuckey D.C. (2017) Removal of selected pharmaceuticals in an anaerobic membrane bioreactor (AnMBR) with/without powdered activated carbon (PAC). *Chem. Eng. J.* 321, 335–345

[18] Abargues, M.R., Ferrer, J., Bouzas, A., Seco, A. (2013). Removal and fate of endocrine disruptors chemicals under lab-scale posttreatment stage. Removal assessment using light, oxygen and microalgae. *Bioresour. Technol.* 149, 142-148

[19] Peng J., Wang G., Zhang D., Zhang D., Li X. (2016). Photodegradation of nonylphenol in aqueous solution by simulated solar UV-irradiation: The comprehensive effect of nitrate, ferric ion and bicarbonate. *J. Photochem. Photobiol. A-Chem.* 326, 9–15

[20] Rajendran R.K., Huang S.L., Lin C.C., Kirschner R. (2017). Biodegradation of the endocrine disrupter 4-tert-octylphenol by the yeast strain *Candida rugopelliculosa* RRKY5 via phenolic ring hydroxylation and alkyl chain oxidation pathways. *Bioresour. Technol.* 226, 55–64

[21] de la Fuente L., Acosta T., Babay P., Curutchet G., Candal R., Litter M.I. (2010). Degradation of Nonylphenol Ethoxylate-9 (NPE-9) by Photochemical Advanced Oxidation Technologies. *Ind. Eng. Chem. Res.* 49, 6909–6915

[22] Kohtani S., Koshiko M., Kudo A., Tokumura K., Ishigaki Y., Toriba A., Hayakawa K., Nakagaki R. (2003). Photodegradation of 4-alkylphenols using BiVO₄ photocatalyst under irradiation with visible light from a solar simulator. *Applied Catalysis B: Environ.* 46, 573–586

[23] Box G.E.P., Hunter J.S. (1961). The 2k-p Fractional Factorial Designs Part I. *Technometrics*, 3, 311-351.

[24] Moliner-Martinez, Y., Pastor-Carbonell, J.M., Bouzas, A., Seco, A., Abargues, M.R., Campins-Falco P. 2013. Guidelines for alkylphenols estimation as alkylphenol polyethoxylates pollution indicator in wastewater treatment plant effluents. *Anal. Methods* 5, 2209-2217

[25] Writer J.H., Ryan J.N., Keefe S.H., Barber L.B. (2012). Fate of 4-Nonylphenol and 17 β -Estradiol in the Redwood River of Minnesota. *Environ. Sci. Technol.* 46, 860–868

[26] Lam M.W., Tantuco K., Mabury S.A. (2003). PhotoFate: A New Approach in Accounting for the Contribution of Indirect Photolysis of Pesticides and Pharmaceuticals in Surface Waters. *Environ. Sci. Technol.* 37, 899-907.

[27] Jacobs L.E., Weavers L.K., Chin Y.P. (2008). Direct and indirect photolysis of polycyclic aromatic hydrocarbons in nitrate-rich surface waters. *Environ. Toxicol. Chem.* 27, 1643–1648

[28] Zepp R.G., Hoigne J., Bader H. (1987). Nitrate-induced photooxidation of trace organic chemicals in water. *Environ. Sci. Technol.* 21, 443–450

[29] Zuo Y. (2003). Light-induced formation of hydroxyl radicals in fog waters determined by an authentic fog constituent, hydroxymethanesulfonate. *Chemosphere* 51, 175–179

[30] Pocostales J.P., Sein M.M., Knolle W., von Sonntag C., Schmidt T.C. (2010). Degradation of Ozone-Refractory Organic Phosphates in Wastewater by Ozone and

Ozone/Hydrogen Peroxide (Peroxone): The Role of Ozone Consumption by Dissolved Organic Matter. *Environ. Sci. Technol.* 44, 8248–8253

[31] Borowska E., Felis E., Kalka J. (2016) Oxidation of benzotriazole and benzothiazole in photochemical processes: Kinetics and formation of transformation products. *Chem. Eng. J.* 304, 852–863

[32] Franke R., Franke C. (1999). Model reactor for photocatalytic degradation of persistent chemicals in ponds and waste water. *Chemosphere* 39, 2651-2659

[33] Liu X.L., Wu F., Deng N.S. (2003). Photodegradation of 17 α -ethynylestradiol in aqueous solution exposed to a high-pressure mercury lamp (250 W). *Environ. Pollut.* 126, 393-398

[34] Ge L., Deng H., Wu F., Deng N. (2008). Microalgae-promoted photodegradation of two endocrine disrupters in aqueous solutions. *J. Chem. Technol. Biotechnol.* 84, 331–336

[35] Ryan C.C., Tan D.T., Arnold W.A. (2011). Direct and indirect photolysis of sulfamethoxazole and trimethoprim in wastewater treatment plant effluent. *Water Res.* 45, 1280-1286

Figure Captions

Figure 1. Schematic diagram of the reactor system: a) longitudinal and b) cross sections. The treatment combinations were; light, oxygen and microalgae (POM), light and oxygen (PO), light (P), oxygen (O) and light and microalgae (PM).

Figure 2. Schematic diagram of the most common free radicals formation.

Figure 3. Degradation of micropollutants under different conditions; a) POM (light, oxygen and microalgae), b) PO (light and oxygen) and c) O (oxygen) on removal of OP, t-NP, 4-NP and BPA in aqueous solution.

Figure 4. Removal of micropollutants in P experiment.

Figure 5. Evolution of the concentration value of dissolved oxygen (DO) during the PM (light and microalgae) experiment.

Figure 6. Removal of micropollutants in PM experiment. Removal is shown through the variation of relative micropollutants concentration with time.

Figure 7. Kinetic method validation proposed for a) OP, b) t-NP, c) 4-NP and d) BPA.

Tables and Figures

Table 1. Experimental conditions during the first 200 min of experiment. Oxygen (O), light (P) and Microalgae (M) at two levels, NO₃⁻ and organic matter (COD).

Treatment Combination	O (mg O ₂ /L)	P (μE/m ² ·s)	M (cell/L)	O	P	M	NO ₃ ⁻ (mg NO ₃ ⁻ -N/L)	COD (mg COD/L)
POM	8.65±0.15	135	(2.1±1.6)·10 ⁺⁰⁹	+	+	+	3.30±0.05	45.3±0.3
P	1.7±0.2	135	0	-	+	-	3.5±0.3	31.8±0.2
PO	8.15±0.11	135	0	+	+	-	3.08±0.11	31.5±0.4
O	8.11±0.12	0	0	+	-	-	2.92±0.18	32.1±0.2
PM	14.7±0.3	135	(2.1±1.6)·10 ⁺⁰⁹	-	+	+	1.04±0.05	46.1±0.2

Table 2. Observed rate constant, correlation coefficients and half-life parameters for the experiments carried out at 23.5 ± 0.5 °C (s.d., standard deviation).

Experiment	EDC	k_{obs} (min^{-1})	\pm	s.d. (min^{-1})	r^2	$t_{(1/2)}$ (min)
POM	OP	0.036	\pm	0.003	0.997	19.3
	t-NP	0.035	\pm	0.002	0.998	19.8
	4-NP	0.0273	\pm	0.004	0.991	25.3
	BPA	0.0142	\pm	0.004	0.98	48.8
PO	OP	0.0433	\pm	0.013	0.98	16.0
	t-NP	0.034	\pm	0.002	0.998	20.5
	4-NP	0.021	\pm	0.002	0.996	33.4
	BPA	0.033	\pm	0.002	0.998	20.8
O	OP	0.025	\pm	0.002	0.994	27.4
	t-NP	0.028	\pm	0.004	0.995	24.8
	4-NP	0.021	\pm	0.003	0.98	32.5
	BPA	0.021	\pm	0.003	0.98	33.3
P	OP	0.0054	\pm	0.0009	0.98	128.0
	t-NP	0.0058	\pm	0.0009	0.994	120.2
	4-NP	0.011	\pm	0.003	0.96	63.1
	BPA	0.0048	\pm	0.0005	0.98	144.2

Table 3. Pseudo-first order rate constant (min^{-1}) and second order degradation rate constants ($\text{L}\cdot\text{mol}^{-1}\cdot\text{min}^{-1}$) for oxygen and hydroxyl radical at 23.5 ± 0.5 °C (s.d., standard deviation); (n.a., not available).

EDC	k'_{O_2}	± s.d.	k'_{OH}	± s.d.	k_{O_2}	± s.d.	$k_{\text{OH}}^{(*)}$	± s.d.
OP	0.026	± n.a.	$2.6\cdot 10^{-04}$	± n.a.	125	± 31	$2.6\cdot 10^{+11}$	± n.a.
t-NP	0.025	± n.a.	$7.0\cdot 10^{-05}$	± n.a.	121	± 16	$7.0\cdot 10^{+10}$	± n.a.
4-NP	0.016	± n.a.	$6.6\cdot 10^{-03}$	± n.a.	77	± 12	$6.6\cdot 10^{+12}$	± n.a.
BPA	0.018	± n.a.	$5.7\cdot 10^{-04}$	± n.a.	87	± 28	$5.7\cdot 10^{+11}$	± n.a.

(*) The values of k_{OH} were calculated using an estimated concentration of hydroxyl radical of 10^{-15} mol/L

Table 4. Observed rate constant, correlation coefficients and half-life parameters for the PM experiment at 23.5 ± 0.5 °C (s.d., standard deviation).

Experiment	EDC	k_{obs} (min^{-1})	\pm s.d. (min^{-1})	r^2	$t_{(1/2)}$ (min)
PM	OP	0.051	\pm 0.009	0.98	13.5
	t-NP	0.050	\pm 0.008	0.990	13.7
	4-NP	0.045	\pm 0.004	0.990	15.5
	BPA	0.043	\pm 0.004	0.990	15.9

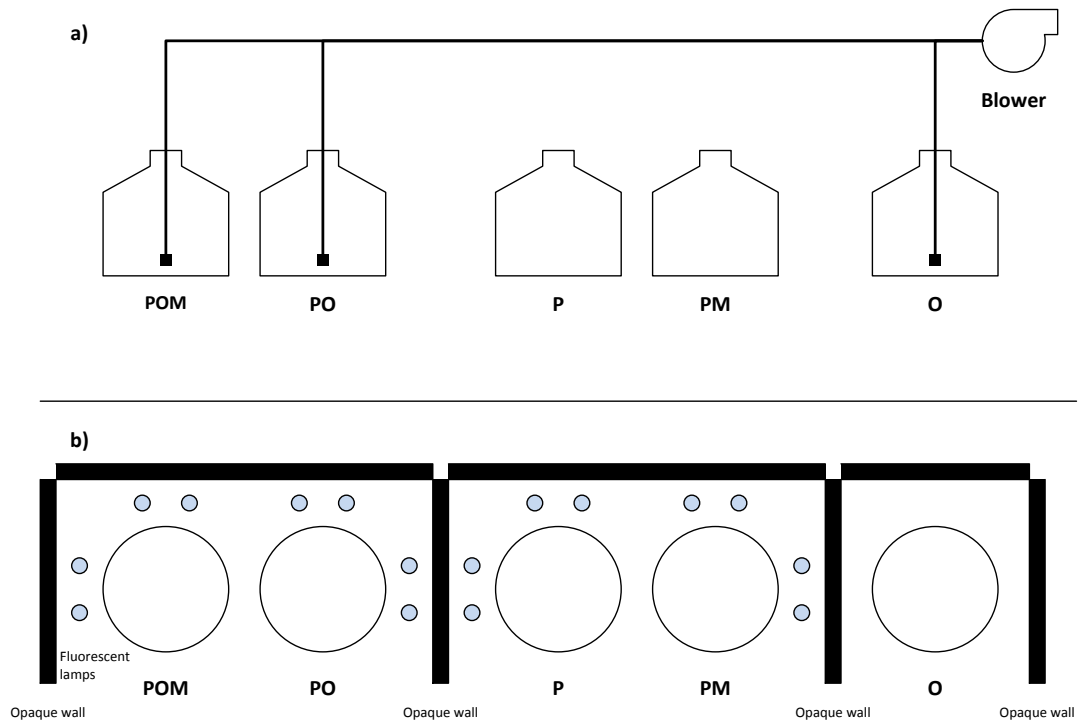


Figure 1. Schematic diagram of the reactor system: a) longitudinal and b) cross sections. The treatment combinations were; light, oxygen and microalgae (POM), light and oxygen (PO), light (P), oxygen (O) and light and microalgae (PM).

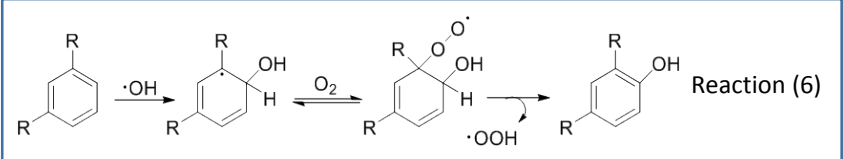
<p style="text-align: center;">Hydroxyl radical ($\cdot\text{OH}$) generation</p>	<p style="text-align: center;">Nitrate ion irradiation</p> <div style="border: 1px solid black; padding: 5px; margin-bottom: 10px;"> $\text{NO}_3^- \xrightarrow{h\nu} \text{NO}_3^{-*} \rightarrow \text{NO}_2 + \cdot\text{O}^- \quad \text{Reaction (1)}$ $\cdot\text{O}^- + \text{H}_2\text{O} \rightarrow \cdot\text{OH} + \text{OH}^- \quad \text{Reaction (2)}$ </div> <p style="text-align: center;">Hydrogen peroxide cleavage</p> <div style="border: 1px solid black; padding: 5px; margin-bottom: 10px;"> $\text{H}_2\text{O}_2 \xrightarrow{h\nu} 2 \cdot\text{OH} \quad \text{Reaction (3)}$ </div> <p style="text-align: center;">Dissolved organic matter (DOM) irradiation</p> <div style="border: 1px solid black; padding: 5px;"> $\text{DOM} \xrightarrow{h\nu} {}^1\text{DOM}^* + {}^3\text{DOM}^* \rightarrow \cdot\text{DOM}$ $\cdot\text{DOM} + \text{O}_2 \rightarrow \cdot\text{DOM}^+ + \text{O}_2^- \quad \text{Reaction (4)}$ $2 \text{O}_2^- + 2 \text{H}^+ \rightarrow \text{H}_2\text{O}_2 + \text{O}_2$ </div>
<p style="text-align: center;">Carbonate radical ($\cdot\text{CO}_3^-$) generation</p>	<div style="border: 1px solid black; padding: 5px;"> $\cdot\text{OH} + \text{CO}_3^{2-} \rightarrow \text{OH}^- + \cdot\text{CO}_3^-$ $\cdot\text{OH} + \text{HCO}_3^- \rightarrow \text{OH}^- + \cdot\text{HCO}_3^- \quad \text{Reaction (5)}$ $\cdot\text{HCO}_3^- \rightleftharpoons \cdot\text{CO}_3^- + \text{H}^+$ </div>
<p style="text-align: center;">Peroxide radical ($\cdot\text{OOH}$) generation</p>	<div style="border: 1px solid black; padding: 5px;">  <p style="text-align: right;">Reaction (6)</p> </div>

Figure 2. Schematic diagram of the most common free radicals formation.

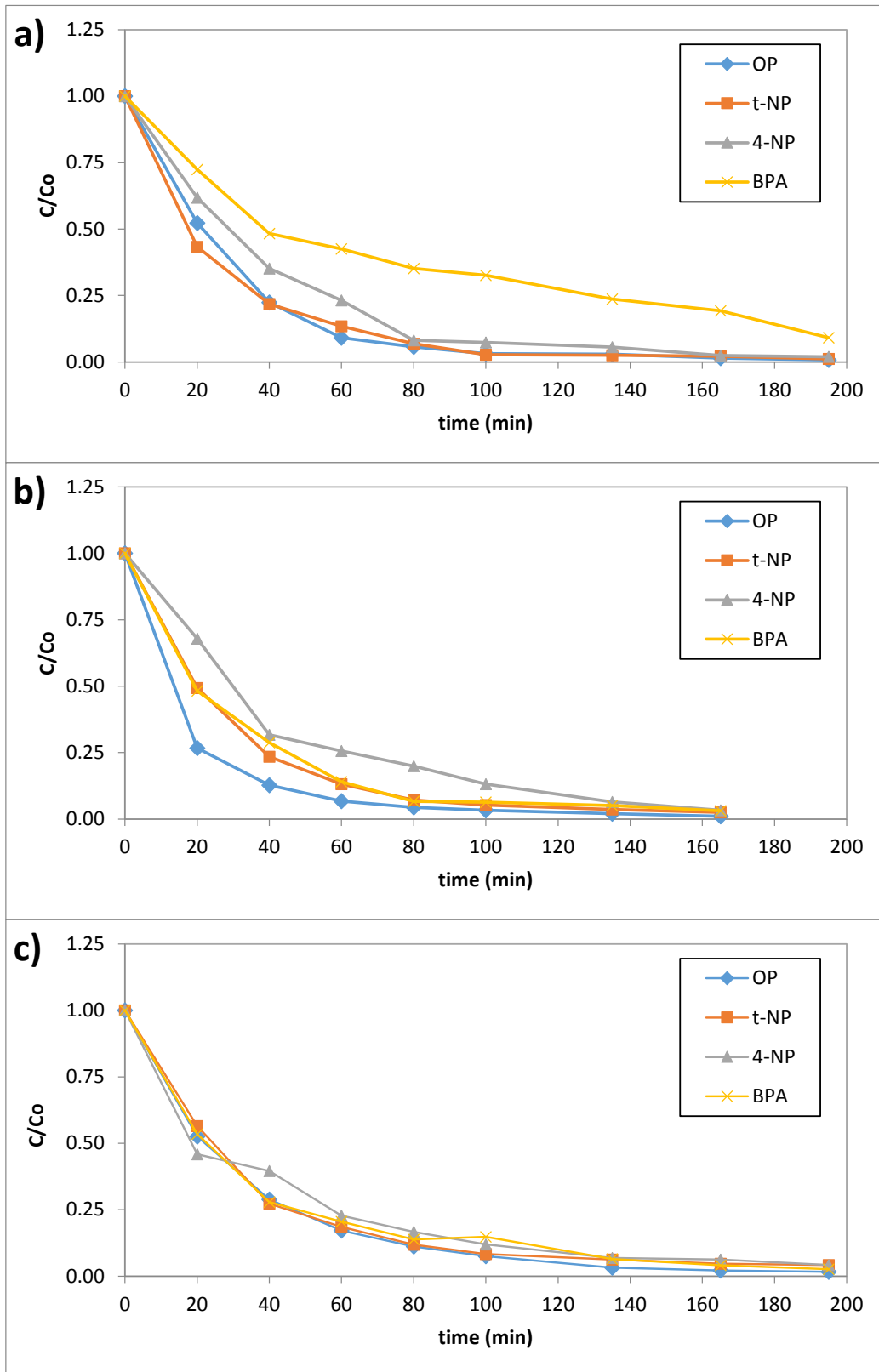


Figure 3. Degradation of micropollutants under different conditions; a) POM (light, oxygen and microalgae), b) PO (light and oxygen) and c) O (oxygen) on removal of OP, t-NP, 4-NP and BPA in aqueous solution.

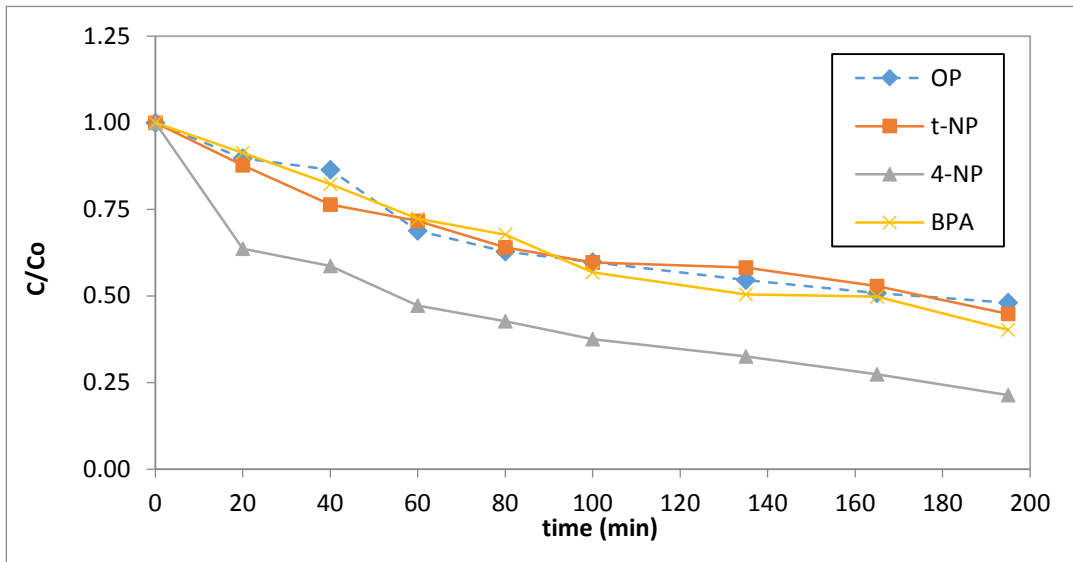


Figure 4. Removal of micropollutants in P experiment.

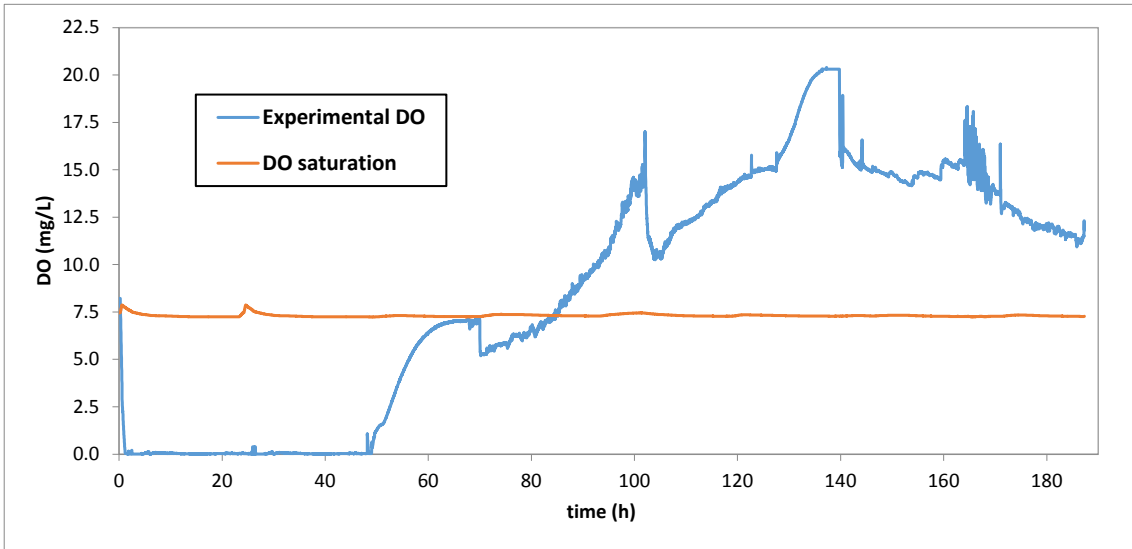


Figure 5. Evolution of the concentration value of dissolved oxygen (DO) during the PM (light and microalgae) experiment.

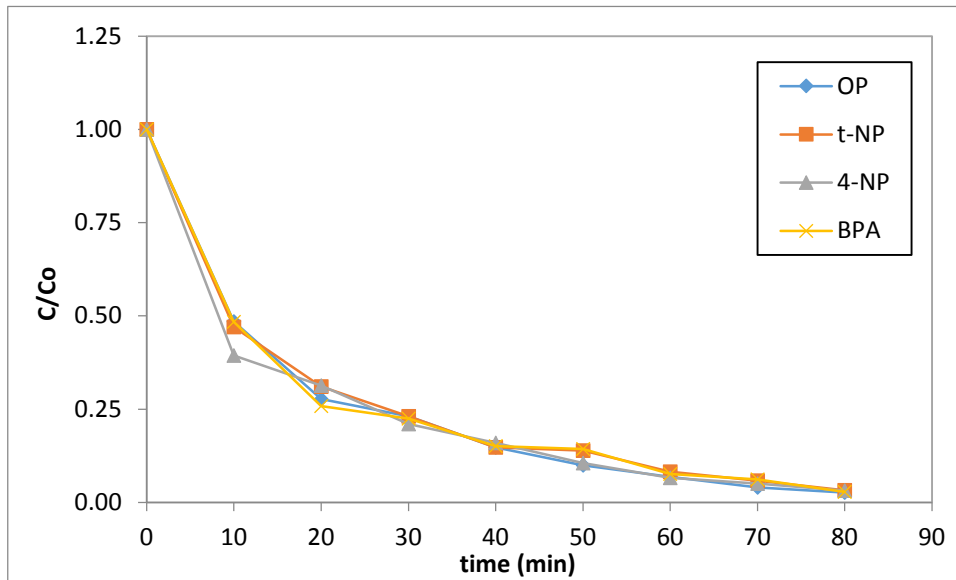


Figure 6. Removal of micropollutants in PM experiment. Removal is shown through the variation of relative micropollutants concentration with time.

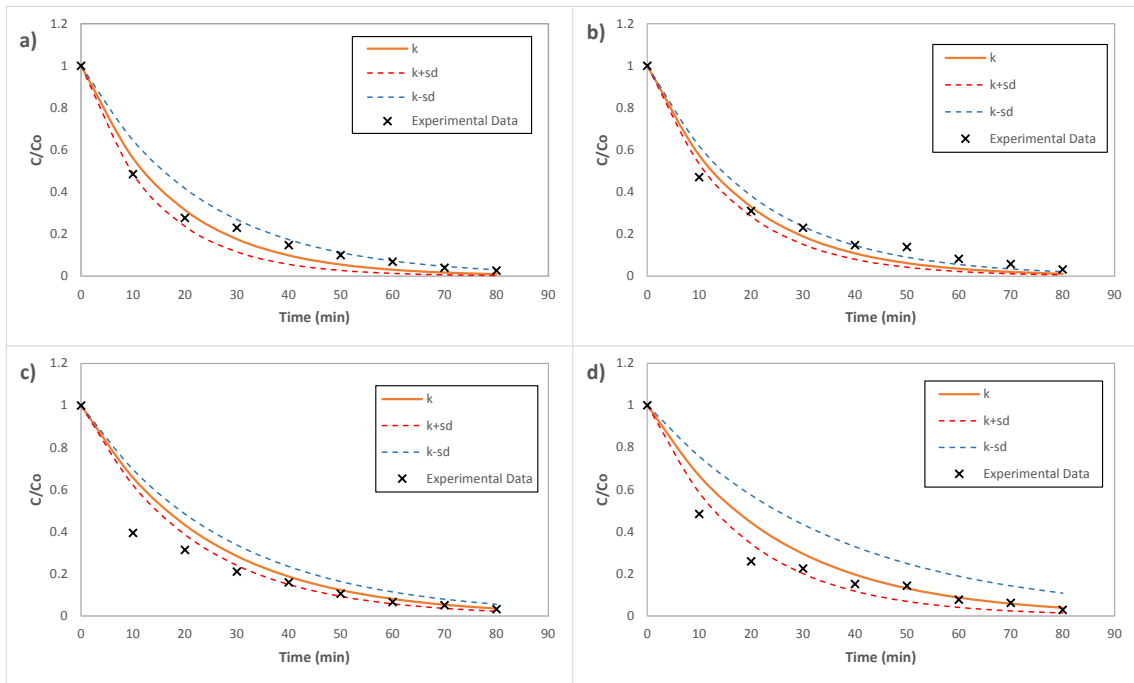


Figure 7. Kinetic method validation proposed for a) OP, b) t-NP, c) 4-NP and d) BPA.

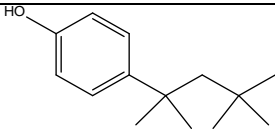
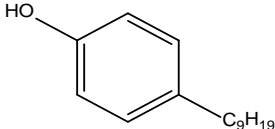
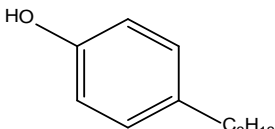
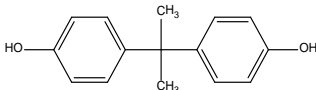
SM1. POM reactor characteristics during the experiment.

	0 h	24 h	48 h	72 h
TSS (mg TSS/L)	71	117	123	180
NH ₄ ⁺ (mg NH ₄ ⁺ -N/L)	41.21	39.75	32.93	23.09
NO ₂ ⁻ (mg NO ₂ ⁻ -N/L)	2.25	2.18	1.96	1.74
NO ₃ ⁻ (mg NO ₃ ⁻ -N/L)	3.26	3.33	2.43	2.10
PO ₄ ³⁻ (mg PO ₄ ³⁻ -P/L)	6.32	5.90	4.29	0.00

SM2. Microbiological composition of the microalgae culture in POM experiment. The concentration of diatoms for the fourth day was not available (n.a.).

	0 h	24 h	48 h	72 h
Chlorophyll A (mg/m ³)	234.5	142.1	288.7	385.4
Diatoms (cell/L)	5.0·10 ⁵	7.6·10 ⁶	1.7·10 ⁷	n.a.
Chlorophyceae (cell/L)	1.7·10 ⁸	6.5·10 ⁸	2.5·10 ⁹	3.4·10 ⁹
Cyanobacteria (cell/L)	2.7·10 ⁸	3.7·10 ⁸	4.1·10 ⁸	4.9·10 ⁸
Total Eukaryotes (cell/L)	1.7·10 ⁸	6.6·10 ⁸	2.5·10 ⁹	3.4·10 ⁹
Diatoms (%)	0.3	1.2	0.7	n.a.
Chlorophyceae (%)	99.7	98.8	99.3	n.a.

SM3. Chemical Structure, Retention time, Quantification and Characteristic Ions of analysed compounds. Log K_{ow} (octanol-water partition coefficient) values for all compounds as predicted by ALOGPS 2.1 software (Virtual Computational Chemistry Laboratory) (<http://www.vcclab.org/>).

Compound	Log K_{ow}	Retention time (min)	Quantification Ion	Characteristic Ions
 <p>4-(1,1,3,3-tetramethylbutyl)phenol (OP)</p>	4.9	8.67	135 (100%)	107 (15%)
 <p>4-nonylphenol (4-NP). C_9H_{19} is a lineal chain.</p>	5.8	10.19	107 (100%)	220 (20%)
 <p>technical-Nonylphenol (t-NP). C_9H_{19} is a branched chain.</p>	5.7	9.20-9.70	135 (100%)	107 (13%)
 <p>Bisphenol A (BPA)</p>	3.6	11.82	213 (100%)	228 (25%), 119 (20%)

SM4. PM reactor characteristics during the experiment.

	0 h	24 h	96 h	120 h	144 h	
TSS	40	52	82	44	250	mg TSS/L
NH ₄ ⁺	28.85	28.33	21.82	21.44	18.11	mg NH ₄ ⁺ -N/L
NO ₂ ⁻	0.00	0.00	0.00	0.00	0.00	mg NO ₂ ⁻ -N/L
NO ₃ ⁻	1.04	0.48	0.73	0.86	0.53	mg NO ₃ ⁻ -N/L
PO ₄ ³⁻	3.73	3.74	0.54	0.60	0.34	mg PO ₄ ³⁻ -P/L

SM5. Microbiological composition of the microalgae culture in PM experiment.

	0 h	24 h	96 h	120 h	144 h
Diatoms (cell/L)	$4.9 \cdot 10^{+6}$	$4.5 \cdot 10^{+6}$	$9.0 \cdot 10^{+6}$	$1.2 \cdot 10^{+7}$	$1.8 \cdot 10^{+8}$
<i>Chlorophyceae</i> (cell/L)	$1.6 \cdot 10^{+7}$	$6.8 \cdot 10^{+7}$	$3.0 \cdot 10^{+8}$	$1.4 \cdot 10^{+9}$	$9.6 \cdot 10^{+9}$
<i>Cyanobacteria</i> (cell/L)	$6.5 \cdot 10^{+7}$	$6.6 \cdot 10^{+6}$	$2.5 \cdot 10^{+7}$	$1.5 \cdot 10^{+8}$	$5.6 \cdot 10^{+8}$
Total Eukaryotes (cell/L)	$2.4 \cdot 10^{+7}$	$7.4 \cdot 10^{+7}$	$3.1 \cdot 10^{+8}$	$1.4 \cdot 10^{+9}$	$9.8 \cdot 10^{+9}$
Diatoms (%)	20.2	6.1	2.9	0.8	1.9
<i>Chlorophyceae</i> (%)	67.1	92.6	95.5	99.2	98.1